Chapter 1
The Geometry of Nature

> *The proper route to an understanding of the world is an examination of our errors about it.*
>
> Euclid (325-265 BC)

Our understanding of nature has been based on the classical geometric figures of smooth line, triangle, circle, cube, sphere, etc. Each of these regular forms can be determined by a characteristic scale. For example, the length of a straight line can be measured with a ruler that has a finer resolution than the entire length of the line. In general, each Euclidean object has a unique value for its characteristics (length, area, or volume). It is also known that when these objects are viewed at higher magnification they do not reveal any new features.

In the real world, however, the objects we see in nature and the traditional geometric shapes do not bear much resemblance to one another. Mandelbrot [2] was the first to model this irregularity mathematically: clouds are not spheres, mountains are not cones, coastlines are not circles, and bark is not smooth, nor does lightning travel in a straight line. Mandelbrot coined the word *fractal* for structures in space and processes in time that cannot be characterized by a single spatial or temporal scale. In fact, the fractal objects and processes in time have multiscale properties, i.e., they continue to exhibit detailed structure over a large range of scales. Consequently, the value of a property of a fractal object or process depends on the spatial or temporal characteristic scale measurement (ruler size) used.

The physiological implications of the fractal concepts are serious since fractal structures and processes are ubiquitous in living things, e.g., the lung, the vascular system, neural networks, the convoluted surface of the brain, ion channel kinetics, and the distribution of blood flow through the blood vessels. Besides, many applications of fractals exist for the morphology of surfaces, e.g., the surface area of a drug particle, surface reactions on proteins. Thus, fractal geometry allows scientists to formulate alternative hypotheses for experimental observations, which lead to more realistic explanations compared to the traditional approaches. These fractal hypotheses can be expressed in terms of quantifying the fractal properties of the system under study as delineated below.

P. Macheras, A. Iliadis, *Modeling in Biopharmaceutics, Pharmacokinetics and Pharmacodynamics*, Interdisciplinary Applied Mathematics 30,
DOI 10.1007/978-3-319-27598-7_1

1.1 Geometric and Statistical Self-Similarity

The most interesting property of fractals is geometric self-similarity, which means that the parts of a fractal object are smaller exact copies of the whole object. Replacement algorithms are used to generate geometric fractals. For example, the Koch curve shown in Figure 1.1 can be produced after four successive replacements according to the following replacement rule: two lines of the same length replace the middle third of the length of the line at each step. Infinite recursions can be applied resulting in a continuous increase of the "line" length by a factor of $4/3$ at each successive step. This continuous ramification of the Koch curve leads to a surprising result if one attempts to measure the length of its perimeter: the length is dependent on the ruler size used for its measurement. In fact, the smaller the ruler size used, the longer the perimeter. Accordingly, when we deal with fractal objects or processes we say that their characteristics (length in this case) "scale" with the measurement resolution.

Similar algorithms for area and volume replacement can be used to create fractals from two- or three-dimensional objects. The fractals shown in Figure 1.2 are called the Sierpinski triangle (gasket) and Menger sponge. They have been generated from an equilateral triangle and a cube, respectively, by applying the following replacement algorithms:

- Sierpinski triangle: At each step an equilateral triangle with area equal to one-quarter of the remaining triangle is removed.
- Menger sponge: At each step one-third of the length of the side of each cube is removed taking care to apply this rule in 3 dimensions and avoiding removal

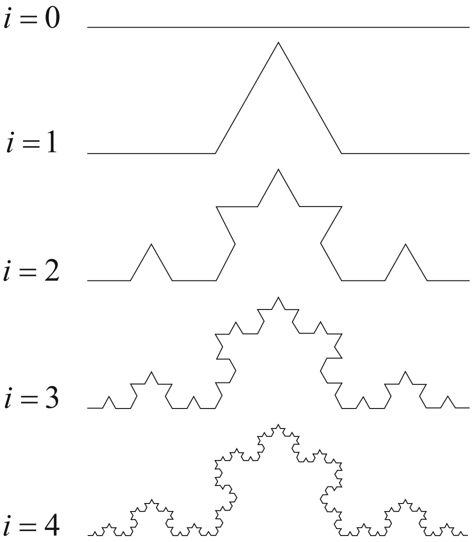

Fig. 1.1 The first four iterations of the Koch curve

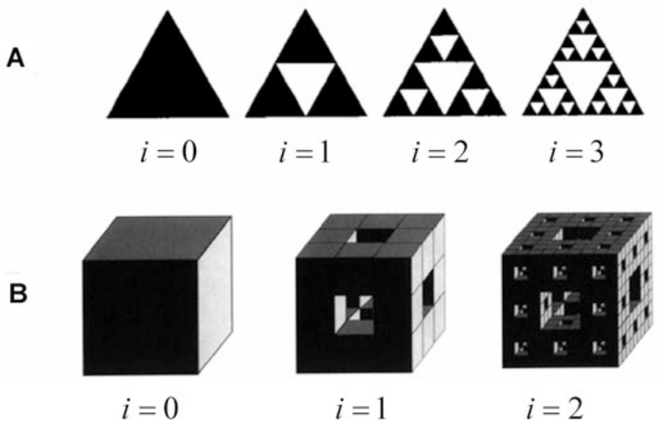

Fig. 1.2 Generation of the (**A**) Sierpinski triangle (gasket) (the first three iterations are shown), (**B**) Menger sponge (the first two iterations are shown) from their Euclidean counterparts

of corner cubes. This means that if the original cube has been constructed from $3 \times 3 \times 3 = 27$ small cubes, after the first iteration 20 small cubes are remaining (6 are removed from the center of the faces and one is removed from the center of the cube).

These line, area, and volume replacement rules give fractal structures (Figures 1.1 and 1.2), which are quite different from the original Euclidean objects. This obvious difference in shape has implications when one considers physical measurements or (bio)chemical processes taking place in Euclidean vs. fractal spaces. For example, surface and/or surface/volume ratios are extremely important for reactions or transport processes taking place at interfaces of different phases like liquid–solid boundaries, e.g., drug dissolution, drug uptake from the gastrointestinal mucosa. In general, objects with fractal surfaces are very efficient for surface reactions.

Replacement rules are expressed mathematically by difference equations, which can be used to generate the fractal structures. These equations are usually called maps and have the form

$$z_{i+1} = g\left(z_i\right), \tag{1.1}$$

where z_i and z_{i+1} are the input and output, respectively, at two successive steps, while the functional form of g in (1.1) depends on the exact features of the recursion process. The discrete nature of (1.1) allows for a recursive creation of the fractal object utilizing the output z_{i+1} as the next input z_i. In this respect, (1.1) operates like a copy machine, which produces the self-similar object in accord with the rule imposed on g.

The replacement rules used for the generation of fractal objects ensure the geometric self-similarity discussed above. However, the fractal objects or processes we encounter in nature are not generated by exact mathematical rules. For example, some biological objects with fractal structure like the venular and arterial tree cannot be characterized by geometric self-similarity; rather they possess statistical self-similarity. The fractal is statistically self-similar since the characteristics (such as the average value or the variance or higher moments) of the statistical distribution for each small piece are proportional to the characteristics that concern the whole object. For example, the average rate at which new vessels branch off from their parent vessels in a physiological structure can be the same for large and small vessels. This is due to the fact that portions of fractal biological objects resemble the whole object instead of being exact copies of the whole. The term *random fractal* is used for these fractal structures to underline their statistical character. Also, statistical self-similarity can be observed when time series data are recorded for physiological processes, e.g., the electroencephalogram or the electrocardiogram. In this case, we speak of statistical self-similarity in time and not in space.

At this point, a distinction should be made between geometrically and statistically self-similar fractals. The pure mathematical basis of geometric fractals does not impose any restriction on the range of application of their scaling laws. In contrast, scaling laws for statistically self-similar fractals adhering to biological objects or processes are subject to the limitations imposed by the physiology and/or the resolution of the measurement technique. In other words, experimental data usually obey scaling laws over a finite range of resolution measurements. This important aspect of scaling laws, with regard to the range of their application, should be carefully considered when one is applying scaling principles for the analysis of experimental data.

1.2 Scaling

The issue of scaling was touched upon briefly in the previous section. Here, the quantitative features of scaling expressed as scaling laws for fractal objects or processes are discussed. Self-similarity has an important effect on the characteristics of fractal objects measured either on a part of the object or on the entire object. Thus, if one measures the value of a characteristic $\theta(\omega)$ on the entire object at resolution ω, the corresponding value measured on a piece of the object at finer resolution $\theta(r\omega)$ with $r < 1$ will be proportional to $\theta(\omega)$

$$\theta(r\omega) = k\theta(\omega), \tag{1.2}$$

where k is a proportionality constant that may depend on r. When statistical self-similarity in time for recordings of an observable is examined, the scale $r\omega$ is a finer time resolution than scale ω. Relation (1.2) reveals that there is a constant ratio k

between the characteristic $\theta(\omega)$ measured at scale ω and the same characteristic $\theta(r\omega)$ measured at scale $r\omega$.

The above-delineated dependence of the values of the measurements on the resolution applied suggests that there is no true value of a measured characteristic. Instead, a scaling relationship exists between the values measured and the corresponding resolutions utilized, which mathematically may have the form of a scaling power law

$$\theta(\omega) = \beta\omega^{\alpha}, \tag{1.3}$$

where β and a are constants for the given fractal object or process studied. Equation (1.3) can be written as

$$\ln\theta(\omega) = \ln\beta + \alpha\ln\omega.$$

This equation reveals that when measurements for fractal objects or processes are carried out at various resolutions, the log–log plot of the measured characteristic $\theta(\omega)$ against the scale ω is linear. Such simple power laws, which abound in nature, are in fact self-similar: if ω is rescaled (multiplied by a constant), then $\theta(\omega)$ is still proportional to ω^{a}, albeit with a different constant of proportionality. As we will see in the rest of this book, power laws, with integer or fractional exponents, are one of the most abundant sources of self-similarity characterizing heterogeneous media or behaviors.

1.3 Fractal Dimension

The objects considered are sets of points embedded in a Euclidean space. The dimension of the Euclidean space that contains the object under study is called the *embedding dimension*, d_e, e.g., the embedding dimension of the plane is $d_e = 2$ and of three-dimensional space is $d_e = 3$.

One is accustomed to associating topological dimensions with special objects: dimension 1 with a curve, dimension 2 with a square, and dimension 3 with a cube. Because there are severe difficulties for the definition of the topological dimension d_t, it is convenient to associate the topological dimension of an object with its *cover dimension* d_o.

A curve in the plane is covered with three different arrangements of disks (Figure 1.3 center). In the right part of the figure there are only pairs of disks with nonempty intersections, while in the center part there are triplets and in the left part even quadruplets. Thus, one can arrange coverings of the curve by only one intersection of each disk with another, and the cover dimension of a line is defined as $d_o = d_t = 1$.

A set of points (Figure 1.3 top) can be covered with disks of sufficiently small radius so that there is no intersection between them. Their covering dimension is

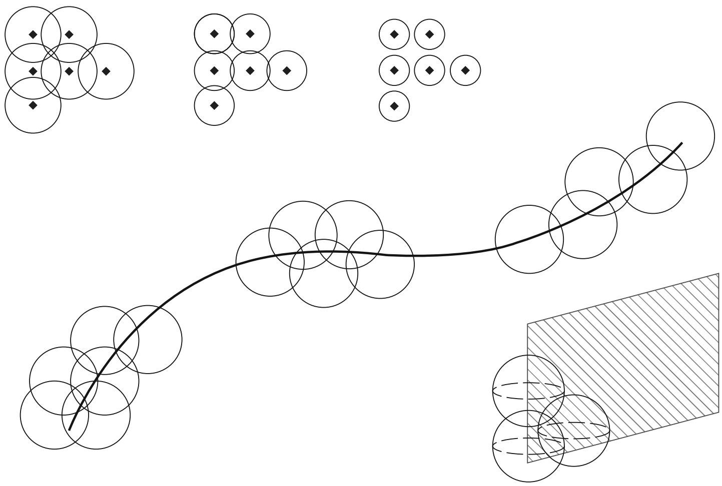

Fig. 1.3 The cover dimension

$d_o = d_t = 0$. A surface (Figure 1.3 bottom) has covering dimension $d_o = d_t = 2$, because one needs at least two overlapping spheres to cover the surface. The same ideas generalize to higher dimensions.

Similarly, the degree of irregularity of a fractal object is quantified with the *fractal dimension*, d_f. This term is used to show that apart from the Euclidean integer dimensions (1 or 2 or 3) for the usual geometric forms, fractal objects have noninteger dimensions. The calculation of d_f using the concept of self-similarity requires in essence the knowledge of the replacement rule, which dictates how many similar pieces m are found when the scale is reduced by a given factor r at each step. Thus, if we count the number m of the exact copies of the entire geometric fractal that are observed when the resolution of scale is changed by a factor of r, the value of d_f can be derived from

$$d_f = \frac{\ln m}{\ln r} \tag{1.4}$$

after logarithmic transformation of

$$m = r^{d_f}. \tag{1.5}$$

For example, the fractal dimension of the Koch curve is 1.2619 since four ($m = 4$) identical objects are observed (cf. levels $i = 0$ and $i = 1$ in Figure 1.1) when the length scale is reduced by a factor $r = 3$, i.e., $d_f = \ln 4/\ln 3 \approx 1.2619$. What does this noninteger value mean? The Koch curve is neither a line nor an area since its (fractal) dimension lies between the Euclidean dimensions, 1 for lines and 2 for areas. Due to the extremely ramified structure of the Koch curve, it covers a portion of a two-dimensional plane and not all of it and therefore its "dimension" is higher than 1 but smaller than 2.

Similarly, the first iteration in the generation of the Sierpinski gasket (Figure 1.2 A) involves the reduction of the scale by a factor $r = 2$ and results in 3 identical black equilateral triangles ($m = 3$); thus, $d_f = \ln 3/\ln 2 \approx 1.5815$. For the Menger sponge (Figure 1.2B), the reduction of the scale by a factor $r = 3$ results in $m = 20$ identical cubes, i.e., $d_f = \ln 20/\ln 3 \approx 2.727$. Both values of d_f are consistent with their dimensions since the Sierpinski gasket lies between 1 and 2, while the Menger sponge lies between 2 and 3.

Equations (1.4) and (1.5) are also valid for Euclidean objects. For example, if one creates $m = 16$ identical small squares in a large square by reducing the length scale by one-fourth, $r = 4$, the value of d_f is $\ln 16/\ln 4 = 2$, which is the anticipated result, i.e., the topological dimension $d_t = 2$ for a plane.

1.4 Estimation of Fractal Dimension

Irrespective of the origin of fractals or fractal-like behavior in experimental studies, the investigator has to derive an estimate for d_f from the data. Since strict self-similarity principles cannot be applied to experimental data extracted from irregularly shaped objects, the estimation of d_f is accomplished with methods that unveil either the underlying replacement rule using self-similarity principles or the power-law scaling. Both approaches give identical results and they will be described briefly.

1.4.1 Self-Similarity Considerations

In principle, the object under study is covered with circles for one- and two-dimensional objects or spheres for three-dimensional objects. This process is repeated using various sizes ω for circles or spheres, while overlapping may be observed. Then, the minimum number of "balls" (circles or spheres) $m(\omega)$ of size ω needed to cover the object is calculated. Finally, the fractal dimension, which in this case is called the *capacity dimension*, d_c is calculated from the relationship

$$d_c = \lim_{\omega \to 0} \frac{\ln m(\omega)}{\ln(1/\omega)}. \tag{1.6}$$

Note that (1.6) relies on the self-similarity concept since the number of identical objects m and the scale factor r in (1.5) have been replaced by the number of "balls" $m(\omega)$ and the reciprocal of the size $1/\omega$, respectively. The limit ($\omega \to 0$) is being used to indicate the estimation of d_c at the highest possible resolution, i.e., as the "ball" size ω decreases continuously.

The reference situation implied in this definition is that at $\omega = 1$, one "ball" covers the object. A clearer definition of d_c is

$$d_c = \frac{\ln\left[m\left(\omega\right)/m\left(1\right)\right]}{\ln\left(1/\omega\right)},$$

or in general, if at $\omega = 1$, k "balls" cover the object,

$$d_c = \frac{\ln\left[m\left(k\omega\right)/m\left(k\right)\right]}{\ln\left(k/k\omega\right)}$$

and

$$d_c = -\frac{\mathrm{d}\ln\left[m\left(\omega\right)\right]}{\mathrm{d}\ln\omega}. \tag{1.7}$$

The capacity dimension tells us how the number of "balls" changes as the size of the "balls" is decreased. This method is usually called *box counting* since the method is implemented in computers with a variety of algorithms utilizing rectangular grids instead of "balls." Dimensions d_f and d_c are quite similar, and the differences between them are usually much smaller than the error of estimates [3].

1.4.2 Power-Law Scaling

When the scaling law (1.3) of the measured characteristic θ can be derived from the experimental data (ω, θ), an estimate of the fractal dimension d_f of the object or process can be obtained as well. In order to apply this method one has first to derive the relationship between the measured characteristic θ and the function of the dimension $g(d_f)$, which satisfies

$$\theta \propto \omega^{g\left(d_f\right)}, \tag{1.8}$$

where ω represents the various resolutions used. Then, the exponents of (1.3) and (1.8) are equated,

$$g(d_f) = \alpha, \tag{1.9}$$

and (1.9) is solved in terms of d_f to derive an estimate for d_f.

The form of the function $g(d_f)$ in (1.9) depends on the measured characteristic θ [4]. For instance:

- When the characteristic is the mass of the fractal object, the exponent of (1.8) corresponds to the value of d_f, $d_f = \alpha$.

- When the characteristic is the average density of a fractal object, $d_f = d_e + \alpha$, where d_e is the embedding dimension.
- For measurements regarding lengths, areas, or volumes of objects, a simple equation can be derived using scaling arguments, $d_f = d_e - \alpha$.

Apart from the estimation of d_f from experimental data for mass, density, and purely geometric characteristics, the calculation of d_f for a plethora of studies dealing with various characteristics like frequency, electrical conductivity, and intensity of light is also based on the exact relationship that is applicable in each case between d_f and the scaling exponent α (1.9).

1.5 Self-Affine Fractals

The replacement rule we have used so far to generate geometric fractals creates isotropic fractals. In other words, the property of geometric self-similarity is the same in all directions. Thus, a unique value for the fractal dimension d_f is being used to quantify an irregular structure. When either the replacement algorithm or the actual physical object exhibits an asymmetry in different directions, then the anisotropic fractal is characterized as a *self-affine fractal*. For example, if one divides a large square into 6 identical small parallelograms and discards 3 of them in an alternate series at each iteration, the result is a disconnected self-affine fractal. Obviously, the unequal horizontal and vertical sides of the parallelograms produced with the successive replacements follow different scaling laws in accord with the dimensions of the sides. The basic difference between self-similarity and self-affinity lies in the fact that self-similar fractals become identical upon simple magnification (classical scaling), while to become identical, self-affine fractals should be scaled by different amounts of the spatial directions. Accordingly, there is no single value of d_f for self-affine fractals; it varies with the ruler size used for measurements. Usually, the box-counting method is applied in conjunction with (1.6) with limits $\omega \to 0$ and $\omega \to \infty$; two estimates for d_f are derived, namely, $d_{f,local}$ and $d_{f,global}$, respectively, and used to characterize a self-affine fractal. Both values indicate limiting values of the fractal dimension: the former is relevant when the size of the boxes decreases infinitely, while the latter corresponds to the largest length scale used for measurements.

1.6 More About Dimensionality

The concept of fractals has helped us to enrich the notion of dimensionality. Apart from the classical systems with dimensions 1, 2, and 3 there are disordered systems with noninteger dimensions.

In the simplest case, a system is called Euclidean or nonfractal if its topological dimension d_t is identical to the fractal dimension d_f. This means $d_t = d_f = 1$ for a curve, $d_t = d_f = 2$ for a surface, and $d_t = d_f = 3$ for a solid. The following relationship holds for the three expressions of dimensionality

$$d_t \leq d_f \leq d_e.$$

Although we have used the value of the fractal dimension d_f as a means to quantify the degree of disorderliness, it is the magnitude of the difference $d_f - d_t$ that in essence reflects how irregular (disordered) the system is. Geometrically speaking, this difference $d_f - d_t$ allows the disordered system to accommodate structure within structure, and the larger this difference is, the more disordered the system.

The above-defined d_f and d_t are *structural parameters* characterizing only the geometry of a given medium. However, when we are interested in processes like diffusion or reactions in disordered media, we need *functional parameters*, which are associated with the notion of time in order to characterize the dynamic behavior of the species in these media. The spectral or fracton dimension d_s and random-walk dimension d_w are two such parameters, and they will be defined in Section 2.2.

1.7 Percolation

The origins of percolation theory are usually attributed to Flory and Stockmayer [5–8], who published the first studies of polymerization of multifunctional units (monomers). The polymerization process of the multifunctional monomers leads to a continuous formation of bonds between the monomers, and the final ensemble of the branched polymer is a network of chemical bonds. The polymerization reaction is usually considered in terms of a lattice, where each site (square) represents a monomer and the branched intermediate polymers represent clusters (neighboring occupied sites), Figure 1.4 A. When the entire network of the polymer, i.e., the cluster, spans two opposite sides of the lattice, it is called a *percolating cluster*, Figure 1.4B.

In the model of bond percolation on the square lattice, the elements are the bonds formed between the monomers and not the sites, i.e., the elements of the clusters are the connected bonds. The extent of a polymerization reaction corresponds to the fraction of reacted bonds. Mathematically, this is expressed by the probability p for the presence of bonds. These concepts can allow someone to create randomly connected bonds (clusters) assigning different values for the probability p. Accordingly, the size of the clusters of connected bonds increases as the probability p increases. It has been found that above a critical value of $p_c = 0.5$ the various bond configurations that can be formed randomly share a common characteristic: a cluster percolates through the lattice. A more realistic case of a percolating cluster can be obtained if the site model of a square lattice is used with probability $p = 0.6$, Figure 1.5. Notice that the critical value of p_c is 0.593 for the

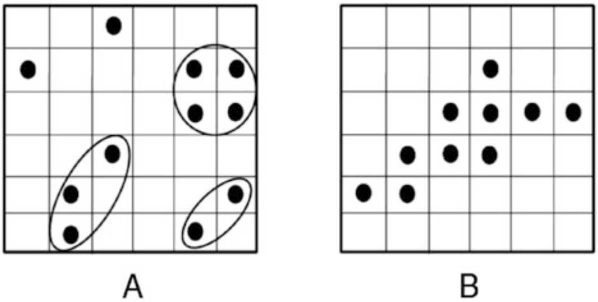

Fig. 1.4 A 6 × 6 square lattice site model. The dots correspond to multifunctional monomers. (**A**) The encircled neighboring occupied sites are clusters (branched intermediate polymers). (**B**) The entire network of the polymer is shown as a cluster that percolates through the lattice from left to right

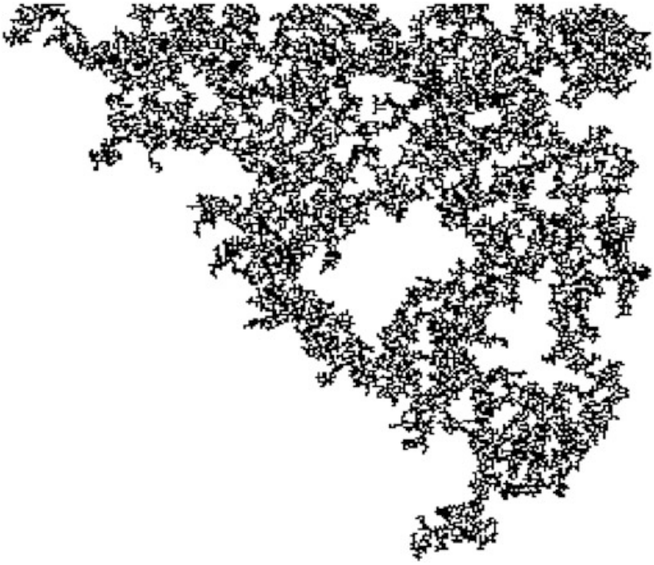

Fig. 1.5 A percolation cluster derived from computer simulation in a 300 × 300 square site model with $p = 0.6$. Only the occupied sites that belong to the percolating cluster are shown

two-dimensional site model. Also, the percolation thresholds vary according to the type of model (site or bond) as well as with the dimensionality of the lattice (2 or 3).

The most remarkable properties of percolation clusters arise from their sudden inception when the bond concentration (probability) reaches the critical threshold value $p = p_c$. At this specific value the emerged cluster spans two opposite sides of the lattice and if one conceives of the bonds as channels, the cluster allows a fluid to flow through the medium from edge to edge. Accordingly, the terms *percolation* and *percolation transition* have been coined in an attempt to capture the sudden change in the geometry and the phase transition. In the same vein, the probability p_∞ that a bond belongs to the percolating cluster undergoes a sharp transition, i.e., $p_\infty = p = 0$ for $p_\infty = p < p_c$, while p_∞ becomes finite following a power law when $p > p_c$

$$p_\infty \propto (p - p_c)^\lambda \,,$$

where λ is an exponent usually called the *critical exponent*. According to the findings in this field of research the critical exponent λ depends exclusively on the dimensionality of the system. This independence from other factors is characterized as *universality*.

Important characteristics of the clusters like the mass q and the typical length ξ of the clusters, usually called the *correlation length*, obey power laws too

$$q \propto |p - p_c|^{-\mu} \,, \qquad \xi \propto |p - p_c|^{-\nu} \,,$$

where μ and ν are also critical exponents. These laws allow reconsideration of the fractal properties of the clusters. According to the last equation the clusters are self-similar as long as the length scale used for measurements is shorter than ξ. For example, the giant cluster shown in Figure 1.5 is a random fractal and as such has a characteristic value for its fractal dimension d_f. However, the calculation of the fractal dimension for the percolating cluster of Figure 1.5 should be performed with radii ρ shorter than ξ. In other words, when $\rho < \xi$ the self-similar character of the cluster is kept and the scaling law holds. Indeed, when the box-counting method is applied, the scaling law $q \propto \rho^{1.89}$ between the mass q (calculated from the mass of ink or equivalently from the number of dots) and the radius ρ of the box is obtained. This means that $d_f = 1.89$ for the percolating cluster of Figure 1.5 since the characteristic measured is the mass for various radii ρ, and no further calculations are required in accord with (1.8). On the contrary, for measurements with $\rho > \xi$, self-similarity no longer exists.